Discrete-state model of coupled ion permeation and fast gating in ClC chloride channels

2008 J. Phys. A: Math. Theor. 41 115001

(http://iopscience.iop.org/1751-8121/41/11/115001)

IOP PUBLISHING JOURNAL OF PHYSICS A: MATHEMATICAL AND THEORETICAL

J. Phys. A: Math. Theor. **41** (2008) 115001 (15pp) doi:10.1088/1751-8113/41/11/115001

Discrete-state model of coupled ion permeation and fast gating in ClC chloride channels

Rob D Coalson

Department of Chemistry, University of Pittsburgh, Pittsburgh, PA 15260, USA

Received 23 November 2007, in final form 1 January 2008
Published 4 March 2008
Online at stacks.iop.org/JPhysA/41/115001

Abstract

A simple discrete-state model of ion permeation through a channel protein is considered in which the flow of ions through the open channel is coupled to the opening/closing of a gate by virtue of configurational changes in a particular pore-lining amino acid residue. The model is designed so as to represent essential features of ClC chloride channels, in which a particular glutamate residue (E148 in bacterial ClC channels) is thought to switch from a conformation that is pinned back (away from the pore itself) to one where this side group blocks the channel at a Cl^- binding site. Thus, competition between the gate residue and Cl^- ions for this site leads to interesting kinetics, such as the saturation of the gate closing time with increasing concentration of internal Cl^- concentration. Analysis of the model proposed here shows that it can account for many qualitative features of ion channel permeation and gate closing rates in ClC-type channels observed experimentally and in recent computer simulations of these processes.

PACS numbers: 82.20.Nk, 82.20.Uv, 83.10.Mj, 87.14.ep, 87.15.hj

(Some figures in this article are in colour only in the electronic version)

1. Introduction

The primary function of the ClC family of ion channels is to regulate the flow of Cl^- across cell membranes, thus controlling a variety of important physiological functions such as skeletal muscle excitability (ClC-1), renal and intravascular transport (ClC-K and ClC-5) and cell volume regulation (ClC-2 and ClC-3). The presence of a double-barreled channel was first suggested by electrophysiological recordings from Torpedo electroplax ClC-0 channel [1] and was recently confirmed by x-ray crystallography [2, 3]. Opening and closing of these two pores appear to be regulated by two distinct mechanisms, corresponding to a fast and a slow gate. Slow gating involves structural changes of both monomers and thus opens or closes both pores simultaneously. The slow gate operates on a time scale of seconds. Fast gating is controlled separately by each individual pore and occurs on a time scale of milliseconds. It

was observed experimentally that both gating mechanisms are regulated by the concentration of Cl^- ions in the bathing solutions abutting the channel entrance on the intracellular and the extracellular sides of the membrane [4–6]. Changing the concentrations of Cl^- on the two sides of the membrane affects the fast gating process in different ways. Increasing the extracellular concentration increases the rate of fast gate opening but has little effect on the closing rate [4, 6–8]. In contrast, increasing the intracellular concentration reduces the rate of fast gate closing but has a much smaller effect on the rate of fast gate opening [4, 9]. Thus, it was suggested that the opening and closing of the fast gate are coupled to ion permeation and controlled via two different mechanisms. To explain the dependence of the fast gate closing rate on the internal Cl^- concentration, Chen *et al* proposed a foot-in-the-door mechanism [4, 9], according to which a permeating Cl^- ion blocks the fast gate from closing by occupying a binding site that would be occupied by the fast gate in the closed state. Dutzler *et al* [2, 3] presented a structural basis for this mechanism and suggested that the permeant Cl^- ions compete with the carboxyl group of the E148 side chain for the binding site located closest to the extracellular side. Recently, Accardi and Miller [10] have demonstrated that the EcClC protein whose x-ray crystal structure was resolved by Dutzler *et al* [2, 3] is actually an H^+–Cl^- exchange transporter, not a passive ion channel. However, these homologous bacterial ClC protein structures have been successfully utilized to rationalize electrophysiological behavior of several ClC-type ion channels [3, 10, 11] and there is strong evidence to support conservation of structure and function among ClC family members [12–14]. The availability of the crystal structures of bacterial ClC proteins [2, 3] has sparked numerous theoretical studies of Cl^- conduction mechanism as well as that of the fast gating in both prokaryotic and eukaryotic pores [15–24]. Of particular relevance here is a recent Brownian dynamics simulation study [24] which has provided a variety of kinetic insights into the 'foot-in-the-door' mechanism of fast gate closure in ClC channels.

In [24], a rigid cylindrically symmetrical model of the open ClC-0 channel was constructed based on available structural, electrophysiological and biochemical data. Permeation of ions was simulated at the Brownian dynamics level (i.e., the high friction limit of the Langevin equation [25]). The single ion potential of mean force (the effective potential in which each ion moves, neglecting Coulombic interactions between pairs of charges) was chosen so as to reproduce essential features gleaned from the x-ray crystal structure, including the location of three Cl^- binding sites located within the channel. These binding sites are generally denoted as $S_{\rm int}$, $S_{\rm cen}$ and $S_{\rm ext}$, as indicated in figure 1. As already noted, x-ray crystal structural data as well as biochemical evidence strongly suggest that the E148 residue near the extracellular entrance to the channel can swing into the pore and occupy the site $S_{\rm ext}$. To model this process in a tractable fashion, the gate was represented in [24] as a spherical particle attached to a pivot rod that allowed it to swing between two energetically stable states, one pinned back away from the channel pore (thus allowing ions to pass) and another in which the gate particle occupies the $S_{\rm ext}$ site of the channel (thus preventing a chloride ion from occupying this site and effectively closing the channel). The gate particle executed Brownian dynamics along a 1D angular coordinate, coupling to the dynamics of the ions via an excluded volume potential (i.e., the gate particle was not allowed to overlap with a Cl^- ion). The simulations reported in [24] were in good qualitative agreement with experimental observations of the gating dynamics experimentally observed in this channel, and in particular were consistent with the 'foot-in-the-door' mechanism of coupled ion permeation-gate closing previously proposed by Chen *et al* [4, 9]. In the BD simulations, as in the experiment, the time taken by the gate to close was found to increase as the concentration of Cl^- in the internal reservoir increased (all other factors being unchanged) and, furthermore, to saturate to a maximum value at high $[Cl^-]_{\rm int}$.

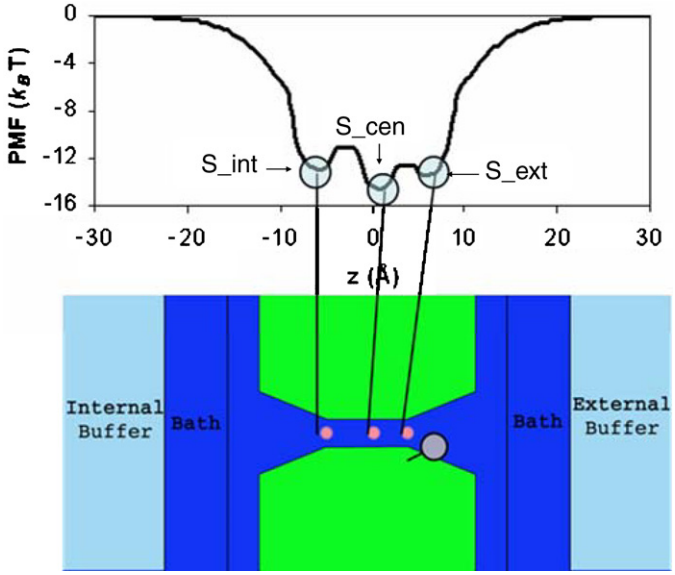

Figure 1. Three-site model of ClC channel ion permeation coupled to fast gate motion.

The results obtained from the 3D BD investigation in [24] strongly suggest the applicability of a discrete-state model to describe the competition between the fast gate in ClC and permeation of Cl^- through the open channel. That is, we define a state of the system as the occupation of the three binding sites by an allowed combination of Cl^- ions and the gate particle, with the restriction that no site can be occupied by more than one particle. Referring to figure 1, it is easy to see that there are exactly 12 such states (including the state in which all three sites are unoccupied). These states then form the basis for a system of 12 kinetic master equations (KMEs) [25], with each pair of states connected by an appropriate rate constant.

The goal of the present paper is to develop a simple discrete-state model of the type just described and show that it does account qualitatively for the major results obtained in the full 3D BD simulations. Since we shall not attempt a quantitative comparison with experiments on ClC channels here, we shall actually analyze a somewhat simpler model than that implied by figure 1, namely, one in which there are only two binding sites in the channel. Specifically S_{cen} and S_{ext} are considered (i.e., the site S_{int} is removed from the model). This model has most of the essentials of a three-site model, for example: (i) competition between permeant Cl^- ions and the gate particle for the S_{ext} site and (ii) influence on Cl^- or gate particle occupancy of S_{ext} by a Cl^- ion occupying a neighboring internal site in the pore. The two-site model of course has the advantage of simplicity: now there are only six states in the model (again, including the state in which both sites in the channel are unoccupied). In section 2 we focus on the properties of the open-channel model, i.e., two Cl^- binding sites with the gate 'pinned back': we briefly consider ion permeation through the open channel and show that it shows the expected (Michaelis–Menten type [26]) saturation behavior as internal $[Cl^-]$ is increased. In section 3, we expand the model to include the gate closing/opening process. We show that it predicts gate closing kinetics which are consistent with Chen *et al*'s foot-in-the-door mechanism [4, 9]. Furthermore, it provides a concrete analytical underpinning for a heuristic approximation considered in [24] that connects the rate of gate closing of the channel to the probability that the open channel is occupied by a Cl^- ion. Section 4 considers the effect of a

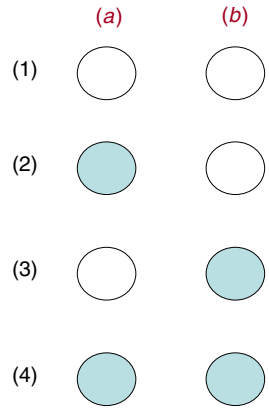

Figure 2. Four-state model of ion permeation through the open ClC channel. The two binding sites a and b are indicated. Note that the intracellular reservoir is to the left of site a and the extracellular reservoir to the right of site b.

charged versus an uncharged gate particle. (It is not known for certain, experimentally, if the gate is charged or uncharged; therefore, it is of interest to consider both possibilities.) Finally, discussion and conclusions are presented in section 5.

2. Discrete-state model of ion permeation through an open two-site channel

For reasons outlined in the introduction we consider here a two-site model of a ClC-like pore: that is, we remove the S_{int} site from the more realistic three-site model of ClC schematized in figure 1, retaining the S_{cen} and S_{ext} sites in the model to be analyzed in this paper. We assume in our idealized model that a Cl^- ion can only occupy one of the two sites (denoted in what follows as a and b) inside the channel pore. Site a is adjacent to the intracellular region of the channel. Site b is adjacent to the extracellular region. In addition to a Cl^- ion, site b can also be occupied by the side chain of E148, which may be thought of in our simplistic picture [24] as an effective spherical particle. The gate particle and Cl^- ions compete for occupation of this site. Thus site b plays the role of S_{ext} in the real ClC channel.

Let us begin with the two-site model of the open channel, in the absence of complications due to fast gate closing. The properties of ion permeation through this channel will play an important role in analyzing the gate closure kinetics in the corresponding channel-gate system.

2.1. Kinetic equations and steady state ion occupation probabilities in the open channel

Figure 2 illustrates the basic model. There are four possible states:

(1) No ions in the channel.
(2) An ion occupies site a; no ion occupies site b.
(3) No ion occupies site a; an ion occupies site b.
(4) An ion occupies site a; an ion occupies site b.

Transitions can be made between these states with appropriate rate constants. We assume (reasonably) that transitions involving motion between nonadjacent sites or concerted motions of two or more ions are disallowed. For simplicity, we also assume that the concentration of Cl^- in the extracellular reservoir is zero, so that this reservoir becomes a sink: it can accept

ions from the channel, but not inject them into it. By contrast, we assume that there is a finite concentration of Cl^- in the internal reservoir. Rate constants corresponding to injection of a Cl^- ion from this reservoir into the a site of the channel are proportional to $[Cl^-]_{int} \equiv c_0$. (Although it is possible to analyze the case where the Cl^- concentration in the extracellular reservoir is non-zero without undue difficulty, the experiments of Chen *et al* which were modeled in [24] correspond to the situation where the external Cl^- concentration is essentially zero.)

Using the notation k_{mn} to denote the rate constant for a transition from state m to state n, we then have the following non-zero rate constants in this model:

k_{12}: injection rate from reactant well into empty channel. We will assume that this rate is proportional to the concentration of Cl^- in the reactant reservoir. Thus, we will take $k_{12}(c_0) = \alpha_{12}c_0$, where α_{12} is a constant.
k_{21}: rate of retreat of an ion occupying site a (with site b unoccupied) into the reactant reservoir.
k_{31}: rate of permeation via state 3.
k_{23}: rate of hopping of an ion from site a into (initially empty) site b.
k_{32}: rate of hopping of an ion from site b (with site a initially empty) to site a.
k_{42}: rate of permeation via state 4.
k_{34}: rate of injection from the reactant reservoir into channel with site a initially unoccupied, but site b occupied. Again, we take $k_{34}(c_0) = \alpha_{34}c_0$, where α_{34} is a constant.
k_{43}: rate of retreat of an ion in site a into the reactant reservoir (site b being occupied).

Denoting the population of state j at time t as $p_j(t)$, then the state populations evolve according to [25]

$$d\vec{p}(t)/\mathrm{d}t = \mathbf{w}\vec{p}(t) \tag{1}$$

with the 4×4 matrix of conditional transitional probabilities $\mathbf{w}$ given explicitly by

$$\mathbf{w} = \begin{pmatrix} -k_{12} & k_{21} & k_{31} & 0 \\ k_{12} & -(k_{21}+k_{23}) & k_{32} & k_{42} \\ 0 & k_{23} & -(k_{31}+k_{32}+k_{34}) & k_{43} \\ 0 & 0 & k_{34} & -(k_{43}+k_{42}) \end{pmatrix}. \tag{2}$$

The solution to equation (1) can be composed from the eigenvectors and eigenvalues of $\mathbf{w}$. Of the four eigenvalues, three are negative and one is zero. The elements of the eigenvector corresponding to the zero eigenvalue gives the relative probabilities to be in states 1–4 at $t = \infty$ ('steady state'). These can be determined analytically. The absolute long-time probabilities are given as $p_j(\infty) \equiv \tilde{p}_j = \bar{p}_j/\mathcal{N}$ with

$$\bar{p}_1 = \frac{1}{k_{12}k_{23}k_{34}}[k_{21}k_{42}(k_{31}+k_{32}+k_{34}) + k_{21}k_{43}(k_{31}+k_{32}) + k_{31}k_{23}(k_{43}+k_{42})] \tag{3}$$

$$\bar{p}_2 = \frac{1}{k_{23}k_{34}}[k_{42}(k_{31}+k_{32}+k_{34}) + k_{43}(k_{31}+k_{32})] \tag{4}$$

$$\bar{p}_3 = (k_{43}+k_{42})/k_{34} \tag{5}$$

$$\bar{p}_4 = 1 \tag{6}$$

and $\mathcal{N} = \sum_{j=1}^{4} \bar{p}_j$. Note that for any unit-normed $\vec{p}(0)$, the probability to be in state j tends to the value of $p_j(\infty)$ given above.

Since two of the rate constants, k_{12} and k_{34}, depend on the concentration of Cl^- in the reactant reservoir c_0, the final state occupation probabilities do too. In particular, consider

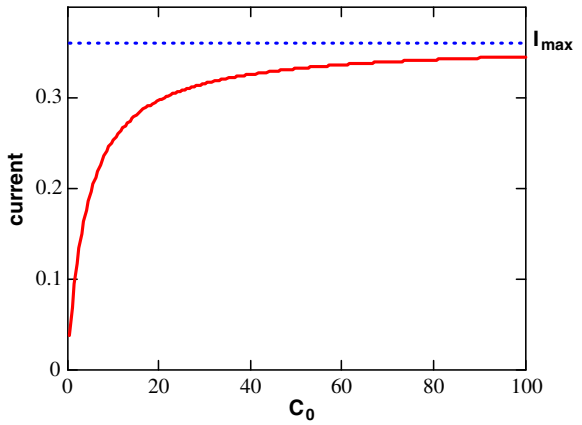

Figure 3. Current of Cl^- ions through the open pore in the four-state model as a function of intracellular Cl^- concentration c_0 (solid line). The asymptotic value corresponding to $c_0 = \infty$, namely $I_{\max} = k_{42}k_{23}/(k_{23} + k_{42})$, is also indicated (dashed line). The following numerical parameters were employed in this calculation: $\alpha_{12} = 0.25, \alpha_{34} = 0.35, k_{32} = 1.4, k_{21} = 0.2, k_{23} = 0.6, k_{31} = 0.3, k_{43} = 0.18, k_{42} = 0.9$.

first the limit that $c_0 \to 0$. As long as there is a mechanism for ions to drain from both sites a and b (which will be the case if none of the other rate constants identified above is zero), then as $c_0 \to 0$, $(p_1(\infty), p_2(\infty), p_3(\infty), p_4(\infty)) \to (1, 0, 0, 0)$, i.e., only the empty state of the channel is occupied. On the other hand, as $c_0 \to \infty$, only states 2 and 4 have non-zero occupation probabilities, namely,

$$p_2(\infty) = \frac{k_{42}}{(k_{23} + k_{42})}; \qquad p_4(\infty) = \frac{k_{23}}{(k_{23} + k_{42})}. \tag{7}$$

Saturation of these state populations as $c_0 \to \infty$ gives rise to saturation in both the current of Cl^- ions that flow through the open channel and, when a gate particle is added to the model (see below), the average rate of channel closing.

2.2. Ion permeation rates through the open channel

Any unit-normed initial state population eventually reaches the steady state values noted above. After short-time transients have decayed, the rate of flow of ions through the channel becomes constant, taking the value (number of ions passing through the channel per second) $I = k_{31}p_3(\infty) + k_{42}p_4(\infty)$. Again, the steady state populations depend on the value of c_0, as detailed above. Based on these steady state populations, we deduce that the ion current goes to 0 at $c_0 = 0$ and saturates to a maximum value of $I_{\max} = k_{42}k_{23}/(k_{23} + k_{42})$ as $c_0 \to \infty$. A generic profile of ion current versus c_0 is shown in figure 3.

3. Coupling of ion permeation to the fast gate

3.1. Details of the model

As noted above, we model the fast gate of the ClC channel as a ball on a pivot arm which in turn can make transitions between two stable states, one corresponding to the gate residue being pinned back away from the channel pore (so that ions can pass through the latter) and the

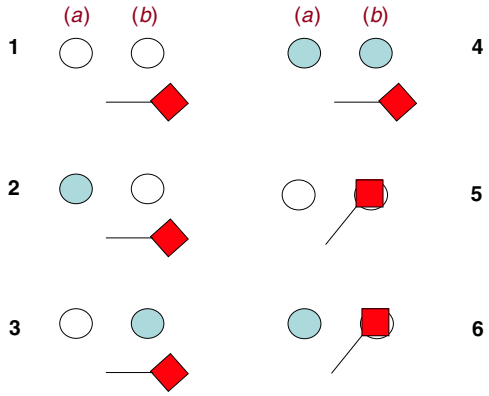

Figure 4. Six-state model of ion permeation coupled to fast gate opening/closing in a model ClC channel. States 1–4 correspond to the open channel, whereas states 5 and 6 correspond to the situation where the gate particle occupies site *b*.

other corresponding to the situation where the fast gate residue occupies site *b* in the channel, thus effectively blocking the passage of Cl^- ions through the channel [2–4, 9]. Thus, we need to alter our definition of the states of the channel and augment the state space in an appropriate manner. In fact, states 1–4 depicted in figure 2 remain states in the augmented state space, provided that we acknowledge that the gate particle is pinned back from the channel (in its 'open' position) in each state. In addition, there are two new states in the model, corresponding to the situation where the gate particle occupies site *b*.

Our model now includes six states, as indicated in figure 4. We must specify non-zero rate constants corresponding to all allowed transitions between any pair of these states. Fortunately, the set of pathways between states 1–4 identified in our original model above (no gate) remains intact, with the understanding that the gate particle stays in its open state (pinned away from the pore) before and after each of these pairwise transitions. We need to add to this set of rate constants additional rate constants that correspond to allowed transitions between states 5 and 6 as well as transitions between members of the state set 1–4 and members of the state set 5 and 6. We shall use the same principle that guided construction of the original state model, namely that only '1 particle moves' are allowed, i.e., concerted moves involving two or more particles (where 'particle' now includes both Cl^- ions and the gate particle) are disallowed. This leads to the following set of additional rate constants:

k_{15}: gate closing rate when site *a* is unoccupied by an ion.
k_{51}: gate opening rate when site *a* is unoccupied by an ion.
k_{26}: gate closing rate when site *a* is occupied by an ion.
k_{62}: gate opening rate when site *a* is occupied by an ion.
k_{56}: rate of ion injection from the intracellular reservoir when site *b* is occupied by the gate particle. As above, we take $k_{56}(c_0) = \alpha_{56} c_0$, where α_{56} is a constant.
k_{65}: rate of ion retraction from site *a* into the intracellular reservoir when site *b* is occupied by the gate particle.

With all non-zero rate constants specified it is easy to construct the 6×6 analog of equation (1) and then to analyze the kinetics of the six-state model (including gate motion), especially once the system has reached steady state. Here we are particularly interested in the following question: given that the gate is open at $t = 0$ how long does it take for it to close on average?

This important quantity can in fact be evaluated using results from the analysis of the four-state model presented above, as is discussed next.

3.2. Gate closing time in the six-state model

Given a system prepared in a configuration where the gate is open (and thus satisfying the condition that $\sum_{j=1}^{4} p_j(0) = 1$), we seek to compute the distribution of survival times (first gate closing events). Equivalently, we can ask what is the probability that the gate has not closed (at all) at time t, i.e., the survival probability $P_S(t)$. For concreteness, consider the case that the system starts from state 1 (no ions in the channel with the gate open). We then consider the time evolution of the subsystem comprised of states 1–4, with states 5 and 6 acting as irreversible probability sinks. That is, the relevant kinetic equations are

$$\mathrm{d}p_1(t)/\mathrm{d}t = -k_{12}p_1 + k_{21}p_2 + k_{31}p_3 - k_{15}p_1 \tag{8}$$

$$\mathrm{d}p_2(t)/\mathrm{d}t = -(k_{21} + k_{23})p_2 + k_{12}p_1 + k_{32}p_3 + k_{42}p_4 - k_{26}p_2 \tag{9}$$

$$\mathrm{d}p_3(t)/\mathrm{d}t = -(k_{31} + k_{32} + k_{34})p_3 + k_{23}p_2 + k_{43}p_4 \tag{10}$$

$$\mathrm{d}p_4(t)/\mathrm{d}t = -(k_{43} + k_{42})p_4 + k_{34}p_3. \tag{11}$$

Again, these are simply the first-order kinetic equations governing the original four-state model (with no gate particle), *augmented* by two sink terms, namely $\mathrm{d}p_1(t)/\mathrm{d}t = \cdots - k_{15}p_1$ and $\mathrm{d}p_2(t)/\mathrm{d}t = \cdots - k_{26}p_2$. The time evolution implied by these rate equations determines $P_S(t) = \sum_{j=1}^{4} p_j(t)$, from which the distribution of survival times can easily be extracted [27]. In particular, the average survival time τ_S, i.e., the average time that it takes the gate to close, is given by $\tau_S = \int_0^\infty \mathrm{d}t\, P_S(t)$.

The key to further analysis is the presumption (consistent with experimental reality as well as the 3D BD model of [24]) that the rates of gate opening and closing are much smaller than the rates at which ions move through the channel. That is, k_{15} and k_{26} are very small in equations (8) and (9). In this case, the *condition of quasi-steady state holds*, i.e. at each instant in time the relative occupation probability to be in state 1–4 is given by the components of the steady state eigenvector of the four-state model obtained in section 2. Then, the condition of quasi-steady state implies that at any time $p_j(t) \cong \tilde{p}_j P_S(t)$.

Now, adding equations (8)–(11) we obtain the net equation

$$\mathrm{d}P_S(t)/\mathrm{d}t = -k_{15}p_1(t) - k_{26}p_2(t). \tag{12}$$

Applying the quasi-steady state condition, this becomes

$$\mathrm{d}P_S(t)/\mathrm{d}t \cong -k_{\mathrm{eff}}P_S(t) \tag{13}$$

where $k_{\mathrm{eff}} \equiv k_{15}\tilde{p}_1 + k_{26}\tilde{p}_2$ is evidently an effective rate constant, since equation (13) implies that $P_S(t) \cong \exp(-k_{\mathrm{eff}}t)$ and thus, finally, that $\tau_S \cong 1/k_{\mathrm{eff}}$.

It is of interest to provide some rationalization for the form of the effective gate closing rate constant k_{eff}. Given the quasi-steady state condition, a system started in one of the open-channel states 1–4 cycles rapidly (on the time scale of gate closing) among these four, occupying each one with a frequency consistent with the steady state probabilities $\tilde{p}_j$, $j = 1 - 4$. Thus, the probability of finding the system in state 1 is $\tilde{p}_1$, and from this state the system can make a transition to a closed-gate state, namely state 5, with rate k_{15}. Similarly, the probability of finding the system in state 2 is $\tilde{p}_2$, and from this state the system can make a transition to a closed-gate state, namely state 6, with rate k_{26}. These are the only routes by which the gate can close in the model under consideration, and the overall gate closure rate

k_{eff} is given by the sum of the contributions from each of them. Note in particular that if the rate of transition of the gate particle into site b (thus closing the pore) is the same regardless of whether site a is occupied by a Cl^- ion or not, i.e., $k_{15} = k_{26} \equiv k_0$, then $k_{\text{eff}} = k_0(\tilde{p}_1 + \tilde{p}_2)$. Of course, $(\tilde{p}_1 + \tilde{p}_2)$ is simply the probability that site b is unoccupied by a Cl^-. This can be stated equivalently as $(\tilde{p}_1 + \tilde{p}_2) = 1 - f_{\text{occ}}(c_0)$, where $f_{\text{occ}}(c_0)$ is the fraction of time (i.e., the probability) that site b *is* occupied by a Cl^- ion, which is a direct function of the intracellular Cl^- concentration c_0; hence we can write $k_{\text{eff}} = k_0[1 - f_{\text{occ}}(c_0)]$. This version of the formula emphasizes that the gate particle *attempts* to move from its open configuration (pinned away from the pore) into a configuration where it occupies site b (thus blocking the pore and closing the channel) with a rate k_0 that is independent of Cl^- motion through the open pore. (Physically, k_0 arises from an activated process involving a free energy barrier along an appropriate reaction coordinate [24].) If there is no Cl^- ion in site b then each attempted closure succeeds, while if there *is* a Cl^- ion in the pore, the attempted closure fails: hence the correction factor $[1 - f_{\text{occ}}(c_0)]$.

4. Charged versus uncharged fast gate

Since it is not known for certain whether the glutamate gate residue is protonated or unprotonated in the open-gate configuration under physiological conditions, both possibilities were simulated in the many-body BD simulations presented in [24]. In the case of a -1 charge on the gate (corresponding to the unprotonated form of the glutamate side group), Coulombic forces between the gate particle and all permeant ions were included in the calculation.

As has already been noted, the simulations reported in [24] were in good qualitative agreement with experimental observations of the gating dynamics experimentally observed in this channel, and in particular were consistent with the 'foot-in-the-door' mechanism of coupled ion permeation-gate closing previously proposed by Chen *et al* [4, 9]. In the BD simulations, as in experiment, the time taken by the gate to close was found to increase as the concentration of Cl^- in the internal reservoir increased (all other factors being unchanged) and, furthermore, to saturate to a maximum value at high $[Cl^-]_{\text{int}}$. For the case where the gate particle was uncharged, direct comparison to a formula obtained via a 'factorized mechanism approximation' was carried out. Specifically, during the time the channel was open, the fraction of simulation time that the S_{ext} site was occupied in the simulation, designated as f_{occ}, was monitored. The accuracy of the approximation $\tau_o(c_0)/\tau_0(0) \cong [1 - f_{\text{occ}}]^{-1}$ compared to $\tau_o(c_0)/\tau_0(0)$ obtained from the full simulations (coupling gate closing to ion permeation) was found to be quite good. As has been discussed above, the simple approximation just noted was based on the following heuristic argument: attempted closing of the gate particle is controlled in the absence of coupling to ion permeation by a 1D barrier crossing process associated with the gate particle potential. This gives rise to a 'bare' closure rate k_0. When ions are moving through the channel, attempted gate closures may be blocked by the presence of a Cl^- ion in the S_{ext} site. The higher the probability of S_{ext} occupation by Cl^- the more likely the blockage will occur; thus the bare rate constant should be reduced roughly by the factor $[1 - f_{\text{occ}}]$.

The kinetic model developed in the present work leads to the same approximation, derived in a more rigorous fashion from the relevant first-order kinetic equations of the model. In particular, if the gate is uncharged the occupation of site a of the model should not have a strong affect on the effective potential experienced by the closing gate particle, i.e., it is reasonable to take $k_{15} = k_{26} \equiv k_0$. Then, as discussed in section 3, $\tau_o(c_0)/\tau_0(0) \cong [1 - f_{\text{occ}}(c_0)]^{-1}$, with $f(c_0) \equiv \tilde{p}_3 + \tilde{p}_4$ being the average probability that site b is occupied by a Cl^- ion while the gate is open.

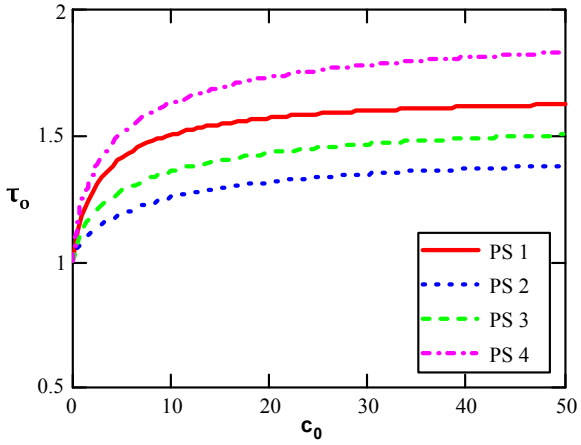

Figure 5. Open time τ_0 versus internal Cl^- concentration c_0 for parameter sets (PSs) 1–4.

The case where the gate particle is charged is more complicated to analyze because there are competing physical consequences associated with the electrostatic repulsions between the charged gate particle and permeating ions. On one hand, the negative charge of the gate particle tends to drive Cl^- ions out of S_{ext}, thus decreasing f_{occ} and increasing the probability of gate closure (i.e., reducing τ_o). On the other hand, the repulsion between the negative gate particle and other ions in the channel adds an additional force that works against gate closure (which would increase τ_o). In fact, for the 3D many-body system studied in the BD simulations of [24] the first factor had a larger impact on the gate closure kinetics, i.e., for the same value of c_0, it was found that τ_o *de*creased when the gate particle was charged (relative to the uncharged gate particle case). The kinetic state model developed in the present work can accommodate all these effects and qualitatively reproduce the behavior found in the full 3D simulations.

To show this, we consider the effect of charging the gate particle upon the rate constants of our two-site ClC-like kinetic model. The repulsion between the negatively charged gate particle in its open state configuration (pinned away from the channel) will tend to drive Cl^- ions back from site b toward the intracellular side of the channel: thus, relative to the case of the uncharged gate, k_{32} and k_{43} will increase, while k_{23} will decrease. These rate constant shifts will act to reduce the average Cl^- occupancy of site b and thus promote gate closure. (According to the allowed transitions of the model, there is no direct pathway to gate closure if site b is occupied.) In the absence of any change in k_{26} (which *is*, in fact, expected to take place: see below), the changes in k_{32}, k_{43} and k_{23} just noted will lead to a decrease in τ_o for the same value of c_0. This is illustrated in figure 5 for the data sets:

(i) Parameter set 1, uncharged gate: $\alpha_{12} = 0.25, \alpha_{34} = 0.35, k_{21} = 0.2, k_{23} = 0.6, k_{32} = 1.4, k_{31} = 0.3, k_{43} = 0.18, k_{42} = 0.9; k_{15} = k_{26} = 0.0024$.
(ii) Parameter set 2, charged gate, no change in k_{26}: $\alpha_{12} = 0.25, \alpha_{34} = 0.35, k_{21} = 0.2, k_{23} = 0.4, k_{32} = 2.8, k_{31} = 0.3, k_{43} = 0.25, k_{42} = 0.9; k_{15} = k_{26} = 0.0024$.

However, as noted above, the presence of a Cl^- in site a will repel the gate particle in its open state configuration, thus leading to a *de*crease in k_{26}. (k_{15} is not affected by the charge state of the gate particle.) This will tend to retard the gate closure, that is, lead to an increase in τ_0. [Note that in biological reality the presence of Cl^- in the channel may also directly drive

changes in the gate residue protonation state, by changing the effective pKa in the region of the protonation site. Including this effect in our model would require further augmentation of the state space, e.g., to include both protonated and deprotonated forms of the gate particle. Although this is beyond the scope of the present work, it could be incorporated into future refinements of our discrete-state model, as discussed briefly in section 5.] Which of the two effects describe above dominates depends on their relative strength. If the change in k_{26} is sufficiently small, then the reduction in the occupancy of site b will dominate. To see this we consider the rate constant set:

(iii) Parameter set 3, charged gate, small reduction in k_{26}: $\alpha_{12} = 0.25, \alpha_{34} = 0.35, k_{21} = 0.2, k_{23} = 0.4, k_{32} = 2.8, k_{31} = 0.3, k_{43} = 0.25, k_{42} = 0.9; k_{15} = 0.0024, k_{26} = 0.0022$.

Results for the gate open time as a function of c_0 for this case are also shown in figure 5. Because the reduction in k_{26} is small compared to the value utilized in sets (i) and (ii), the effect of reduced occupancy of site b dominates and τ_0 decreases relative to the uncharged gate case, (i), for the same value of c_0. (Note: this figure should be compared to figure 12(a) of [24]. The curves in [24] denoted as neutral gate and negatively charged gate correspond in our figure 5 to parameter sets (i) and (iii), respectively.) However, if the reduction in k_{26} is sufficiently large, the effect of direct repulsion between the gate particle in its open state configuration and Cl^- ions in the channel will dominate, and the overall rate of gate closure will decrease (i.e., τ_0 will increase) relative to the uncharged gate case. This is also shown in figure 5 using the rate constant set:

(iv) Parameter set 4, charged gate, large reduction in k_{26}: $\alpha_{12} = 0.25, \alpha_{34} = 0.35, k_{21} = 0.2, k_{23} = 0.4, k_{32} = 2.8, k_{31} = 0.3, k_{43} = 0.25, k_{42} = 0.9; k_{15} = 0.0024, k_{26} = 0.0018$.

This example shows the various ways in which charging the gate can influence gate closure rates. Again, which effects will dominate depends on the magnitudes of the perturbations of the rate constants in the model. A careful (and, in practice, difficult) application of physico-chemical theory is required to compute these rate constants from an atomistic model of the system or even an idealized many-body model such as was considered in [24]. (Note that any such treatment will naturally build in constraints between rate constants which reflect the details of the underlying free energy profiles [28].) In the case of the model considered in [24], the reduction in Cl^- occupancy of site b (i.e., S_{ext}) was evidently the dominant factor.

In [24], it was shown that one could approximately compensate for the influence of decreased site b occupancy by Cl^- upon the rate of closing of a charged gate particle and thus isolate the effect of electrostatic repulsion of the gate particle by Cl^- ions in the channel, by plotting τ_0 versus the fractional occupancy of the b site $f_{occ}(c_0)$. (In the case of the charged gate, a higher value of c_0 is required to achieve the same value of $f_{occ}(c_0)$.) It was observed in the 3D Brownian dynamics simulations that τ_0 was larger for the charged gate particle than the uncharged gate particle at a particular value of f_{occ}. The same qualitative behavior occurs in the site model considered in the present work. In fact, we show in the appendix that this trend occurs in the present model for any reduction in k_{26} incurred upon charging the gate particle. Numerical results comparing parameter sets (i) and (iii), which correspond most directly to the uncharged gate and charged gate situations, respectively, encountered in [24] (in particular, cf figure 12(b) of that reference) are provided in figure 6.

5. Discussion and conclusions

In this paper, we have analyzed a two-site (six-state) model of the dynamical coupling between the closing of the fast gate of the ClC channel and the permeation of ions through the open

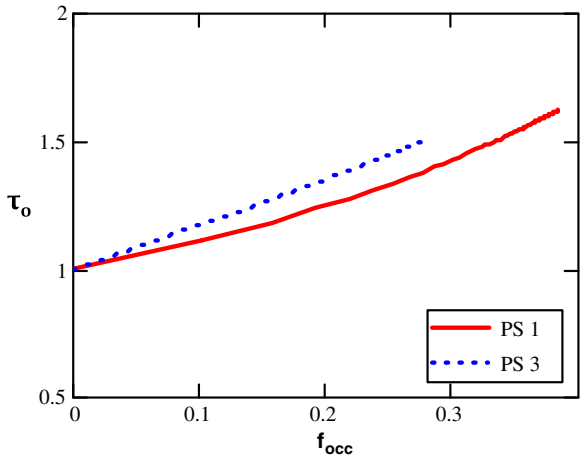

Figure 6. Open time τ_0 versus f_{occ} (fraction of time that site b is occupied by a Cl^- ion) for parameter sets 1 and 3.

channel (as controlled by the concentration of Cl^- in the internal side bathing solution), in order to explain effects observed both in experiments and in recent computer simulations. As explained at the outset, our model represents a considerable simplification of the (exquisitely complex!) ClC protein channel. It should thus be described more properly as a model of a ClC-like channel rather than the ClC channel itself. Nevertheless, this model has been shown to account in a simple and transparent way for the saturation of both the Cl^- ion current flow through the open channel in response to increasing internal [Cl^-] and the rate of closing of the gate as function of the same control parameter. This latter phenomenon, known as the 'foot-in-the-door' mechanism of coupling of ion permeation and gate closing in the ClC channel, is easily represented in a discrete-state model of the type considered herein. A recent many-body Brownian dynamics simulation study which elucidated the same mechanism at a more atomistic level [24] explored the effect of having a charged versus an uncharged gate (represented in that work as a single effective particle which could swing on a pivot arm into and away from the S_{ext} site of the pore). With appropriate choices for the underlying rate constants, the discrete-state model developed in the present work yields results which are qualitatively consistent with the many-body simulations of [24]. An obvious strength of the discrete-state model is the rapidity with which one can compute the kinetic consequences of given rate constants and, consequently, gain insight into the effects of the strengths of the contributions to the various driving forces behind the process, as was demonstrated in our presentation of the effects of gate charging (section 4).

Given the qualitative success of the present model, we will strive in future work to refine it toward more realism. It would be interesting as a proof of principal analysis to attempt to reproduce the many-body BD simulation results of [24] at a *quantitative* level. In addition to an augmentation of the state space as indicated in figure 1 (3 binding sites, 12 states in the model), extraction of appropriate state-to-state rate constants based on the underlying geometry and energetic features of the [24] simulation system is required. From the underlying driving forces, i.e., effective potential governing the single particle move appropriate for each of the state-to-state transitions in the discrete-state model, drift-diffusion theory can be utilized to extract state-to-state rate constants. (For example, given an ion in the S_{int} binding site, the rate of transition of this ion to S_{cen} in the case that the channel is open and otherwise empty can be

computed from the Kramer's formula for the rate of activated crossing over a 1D barrier [25].) This analysis would serve as a check on our ability to extract state-to-state rate constants for a discrete-state model of the type depicted in figure 1 from fundamental physico-chemical principles.

Ultimately, the calculation of such rate constants is only as good as the effective potential energy (or free energy) profiles which they utilize as input. Calculation of such profiles in a real ClC channel is difficult and time consuming. The most rigorous approach for determining the effective potential felt by a Cl^- ion during its motion is to calculate the potential of mean force (constrained free energy) for moving it from one site to the next. This requires large-scale MD simulations of the channel protein, embedding lipid bilayer membrane, and solvent water molecules with a test Cl^- ion fixed at (or harmonically bound to) a particular position in space. Conceptually, it is straightforward to do this, but the development and implementation of accurate techniques to do so remains an active field of research [29, 30]. The treatment of the gate 'particle' requires even more thought, since it is not actually a single particle, but a side group of an amino acid. Thus, an appropriate reaction coordinate (order parameter) for its transformation from open to closed (pore-blocking) states has to be identified. Examination of the coordinates corresponding to the open and closed configurations in the crystal structures of bacterial ClC pores [2, 3] reveals that the dihedral angle $C–C_\alpha–C_\beta–C_\gamma$ changes by ca 90° between the open and closed state structures and that this is the major coordinate change required to morph between the two structures [24]. Thus, it would be reasonable to take this dihedral angle to be the reaction coordinate [23] (effectively identifying it with the angular coordinate utilized in the 3D BD model of [24]).

Finally, it would be interesting to model the effects of gate protonation/deprotonation in a dynamical fashion, by adding more states to the state space and specifying rate constants that connect them. Every state in the model with assumed fixed protonation state of the gate would become two states in the discrete-state model: one for the protonated glutamate state and other for the deprotonated state. Determining rate constants for transformation states from first principles all-atom free energy simulations [29, 30] remains a difficult task [21–23], but as accurate results from such computations become available, protonation/deprotonation rate constants can be estimated, including their dependence on the pH of the external bathing solution. Clearly, there are many steps remaining en route to a quantitatively accurate mapping of the full many-body dynamics of the ClC protein channel system and its environment to a discrete-state model characterized by a modest number of states.

Acknowledgments

The author would like to thank T L Beck, M H Cheng and A B Mamonov for many stimulating discussions on this topic. This work was supported in part by NSF Grant No CHE-0518044 and ARO-MURI Grant No DADD19-02-1-0227.

Appendix

According to the analysis presented in the text, the gate closure time when ions are passing through the channel relative to that when the channel is empty (as is the case when $c_0 = 0$) is given by $\tau_o(c_0)/\tau_o(c_0 = 0) = k_{15}/[k_{15}\tilde{p}_1 + k_{26}\tilde{p}_2]$. For an uncharged gate, we take $k_{15} = k_0 = k_{26}$, i.e., we designate the rate of gate closing in the absence of ions in the channel as k_0 and assume that this gate closure rate is the same if a Cl^- ion occupies site a (because the gate particle is not charged). When the gate is open, there will be some steady

state occupation probabilities of the four gate-open states, which we shall designate here as $\tilde{p}_j^u$, $j = 1-4$ (the superscript u stands for 'uncharged'). If the gate is now charged, we assume that k_{15} does not change relative to the uncharged gate case, i.e. $k_{15} = k_0$, because there are no other charges in the pore region for the charged gate to interact with. However, k_{26} will decrease, i.e., $k_{26}^c < k_0$, because of repulsion between the gate particle and Cl^- ions occupying the channel. (The superscript c designates 'charged'.) Furthermore, because of changes in k_{32}, k_{43} and k_{23} discussed in the text, the occupation probabilities of the four gate-open states will change relative to the uncharged gate case. We will designate the charged gate versions as $\tilde{p}_j^c$, $j = 1-4$.

We are interested in plotting $\tau_o(c_0)/\tau_o(c_0 = 0)$ versus f_{occ}, the fraction of time that site b is occupied by a Cl^- ion while the gate is open. This quantity is given by $f_{\text{occ}} = \tilde{p}_3^u + \tilde{p}_4^u = \tilde{p}_3^c + \tilde{p}_4^c$. This implies that for a given value of f_{occ}, we have $\tilde{p}_3^u + \tilde{p}_4^u = \tilde{p}_3^c + \tilde{p}_4^c$ or, equivalently, $\tilde{p}_1^u + \tilde{p}_2^u = \tilde{p}_1^c + \tilde{p}_2^c$. So, for the uncharged gate:

$$\tau_o^u \big/ \tau_o(c_0 = 0) = k_0 \big/ \left[k_0\left(\tilde{p}_1^u + \tilde{p}_2^u\right)\right]$$

while for the charged gate:

$$\begin{aligned}\tau_o^c \big/ \tau_o(c_0 = 0) &= k_0 \big/ \left[k_0 \tilde{p}_1^c + k_{26}^c \tilde{p}_2^c\right] = k_0 \big/ \left[k_0\left(\tilde{p}_1^c + \tilde{p}_2^c\right) + \left(k_{26}^c - k_0\right)\tilde{p}_2^c\right] \\ &= k_0 \big/ \left[k_0\left(\tilde{p}_1^u + \tilde{p}_2^u\right) + \left(k_{26}^c - k_0\right)\tilde{p}_2^c\right].\end{aligned}$$

Since $\left(k_{26}^c - k_0\right)\tilde{p}_2^c < 0$, then $\tau_o^c > \tau_o^u$ at the same value of f_{occ}.

References

[1] Miller C 1982 Open-state substructure of single chloride channels from torpedo electroplax *Philos. Trans. R. Soc. Lond. B* **299** 401–11

[2] Dutzler R, Campbell E B, Cadene M, Chait B T and MacKinnon R 2002 X-ray structure of a ClC chloride channel at 3.0 A reveals the molecular basis of anion selectivity *Nature* **415** 287–94

[3] Dutzler R, Campbell E B and MacKinnon R 2003 Gating the selectivity filter in ClC chloride channels *Science* **300** 108–12

[4] Chen T Y and Miller C 1996 Nonequilibrium gating and voltage dependence of the ClC-0 Cl-channel *J. Gen. Physiol.* **108** 237–50

[5] Richard E A and Miller C 1990 Steady-state coupling of ion-channel conformation to a transmembrane ion gradient *Science* **247** 1208–10

[6] Pusch M, Ludewig U, Rehfeldt A and Jentsch T J 1995 Gating of the voltage-dependent chloride channel ClC-0 by the permeant anion *Nature* **373** 527–31

[7] Engh A M, Faraldo-Gomez J D and Maduke M 2007 The mechanism of fast-gate opening in ClC-0 *J. Gen. Physiol.* **130** 335–49

[8] Engh A M, Faraldo-Gomez J D and Maduke M 2007 The role of a conserved lysine in chloride- and voltage-dependent ClC-0 fast gating *J. Gen. Physiol.* **130** 351–63

[9] Chen T Y, Chen M F and Lin C W 2003 Electrostatic control and chloride regulation of the fast gating of ClC-0 chloride channels *J. Gen. Physiol.* **122** 641–51

[10] Accardi A and Miller C 2004 Secondary active transport mediated by a prokaryotic homologue of ClC Cl channels *Nature* **427** 803–7

[11] Chen T Y 2003 Coupling gating with ion permeation in ClC channels *Sci STKE 2003* pe23

[12] Estvez R, Schroeder B C, Accardi A, Jentsch T J and Pusch M 2003 Conservation of chloride channel structure revealed by an inhibitor binding site in ClC-1 *Neuron* **38** 47–59

[13] Engh A M and Maduke M 2005 Cysteine accessibility in ClC-0 supports conservation of the ClC intracellular vestibule *J. Gen. Physiol.* **125** 601–17

[14] Lin C W and Chen T Y 2003 Probing the pore of ClC-0 by substituted cysteine accessibility method using methane thiosulfonate reagents *J. Gen. Physiol.* **122** 147–59

[15] Cohen J and Schulten K 2004 Mechanism of anionic conduction across ClC *Biophys. J.* **86** 836–45

[16] Corry B, O'Mara M and Chung S-H 2004 Conduction mechanisms of chloride ions in ClC-type channels *Biophys. J.* **86** 846–60

[17] Allen T W and Chung S-H 2001 Brownian dynamics study of an open-state KcsA potassium channel *BBBA-Biomem.* **1515** 83–91

[18] Bisset D, Corry B and Chung S-H 2005 The fast gating mechanism in ClC-0 channels *Biophys. J.* **89** 179–86
[19] Miloshevsky G V and Jordan P C 2004 Anion pathway and potential energy profiles along curvilinear bacterial ClC Cl pores: electrostatic effects of charge residues *Biophys. J.* **86** 825–35
[20] Bostick D L and Berkowitz M L 2004 Exterior site occupancy infers chloride-induced proton gating in a prokaryotic homolog of the ClC chloride channel *Biophys. J.* **87** 1686–96
[21] Yin J, Kuang J Z, Mahankali U and Beck T L 2004 Ion transit pathways and gating in ClC chloride channels *Proteins: Struct. Funct. Bioinform.* **57** 414–21
[22] Beck T, Yin J, Kuang Z F, Mahankali U and Feng G G 2006 Comment on ion transit pathways and gating in CIC chloride channels *Proteins: Struct. Funct. Bioinform.* **62** 553–4
[23] Kuang J Z, Mahankali U and Beck T L 2007 Proton pathways and H+Cl− stoichiometry in bacterial chloride transporters *Proteins: Struct. Funct. Bioinform.* **68** 26–33
[24] Cheng M H, Mamonov A B, Dukes J W and Coalson R D 2007 Modeling the fast gating mechanism in the ClC-0 chloride channel *J. Phys. Chem.* B **111** 5956–65
[25] van Kampen N 1992 *Stochastic Processes in Physics and Chemistry* (Amsterdam: North-Holland)
[26] Atkins P W and De Paula J 2006 *Atkins' Physical Chemistry* 8th edn (San Francisco, CA: Freeman)
[27] Colquhoun D and Hawkes A G 1981 On the stochastic properties of single ion channels *Proc. R. Soc.* B **211** 205–35
[28] Kim Y C, Wilkström M and Hummer G 2007 Kinetic models of redox-coupled proton pumping *Proc. Natl Acad. Sci.* **104** 2169–74
[29] Beck T L, Paulaitis M E and Pratt L R 2006 *The Potential Distribution Theorem and Models of Molecular Solutions* (Cambridge: Cambridge University Press)
[30] Chipot C and Pohorille A (ed) 2007 *Free Energy Calculations: Theory and Applications in Chemistry and Biology* (Berlin: Springer)